

RSC Advances



This is an *Accepted Manuscript*, which has been through the Royal Society of Chemistry peer review process and has been accepted for publication.

Accepted Manuscripts are published online shortly after acceptance, before technical editing, formatting and proof reading. Using this free service, authors can make their results available to the community, in citable form, before we publish the edited article. This *Accepted Manuscript* will be replaced by the edited, formatted and paginated article as soon as this is available.

You can find more information about *Accepted Manuscripts* in the [Information for Authors](#).

Please note that technical editing may introduce minor changes to the text and/or graphics, which may alter content. The journal's standard [Terms & Conditions](#) and the [Ethical guidelines](#) still apply. In no event shall the Royal Society of Chemistry be held responsible for any errors or omissions in this *Accepted Manuscript* or any consequences arising from the use of any information it contains.

Cite this: DOI: 10.1039/c0xx00000x

www.rsc.org/xxxxxx

ARTICLE TYPE

Intestine-like micro/mesoporous carbon built of chemically modified banana peel for size-selective separation of proteins

Rui-Lin Liu,^{a,b} Fu-Yu Yin^a, Ji-Fang Zhang^a, Jing Zhang^a, and Zhi-Qi Zhang^{*a,b}

Received (in XXX, XXX) Xth XXXXXXXXX 20XX, Accepted Xth XXXXXXXXX 20XX

DOI: 10.1039/b000000x

An intestine-like micro/mesoporous carbon (ILMC) was fabricated by chemically modifying banana peel and used for size-selective separation of proteins. The as-made ILMC has been exemplarily characterized by FTIR, XRD, SEM, TEM, and N₂ adsorption measurements. The adsorption property of ILMC was further evaluated with three different molecular size proteins, cytochrome c, bovine serum albumin and lysozyme, at binary and ternary hybrid solutions, respectively. The results showed that the ILMC is effective and highly selective adsorbent for cytochrome c. This simple and procurable ILMC may be utilized as a potential and promising support for immobilizing bio-macromolecules, and drug delivery and separation.

Introduction

Carbon materials (CMs) with high porosity and large pore volume are widely employed in adsorption and energy storage, and as a carrier for drug delivery system.¹ Extensive methods have been used to fabricate various CMs, including hard and soft templating or activation methods.² Traditional inorganic materials, zeolite and silica, are known templates for casting porous carbon. However, this method is costly, complicated and always involves in highly toxic substances, which hinders its application in large scale production. Interestingly, CMs fabricated from waste biomass have shown extensive attention and promising applications as sorption materials, and others.³ Biomass, because of its inexpensive, easy to obtain, rapid regeneration, and nontoxic, has a qualification as a promising starting material for the synthesis of carbonaceous materials.⁴⁻⁷ Up to now, some processing techniques such as hydrothermal carbonization and direct pyrolysis, have been established for fabricating high quality CMs.^{4,8} But, whether the biomass conversion system is thermochemical or biological, there still doesn't appear to be a satisfactory and optimal process.⁴ Particularly, the application in the separation and adsorption of giant molecules such as proteins is scarce for CMs prepared with low-valued carbon sources.

The adsorption or isolation of proteins from solution onto solid surface has attracted much attention due to its scientific importance and application in many areas, such as biology, medicine and biotechnology.⁹ So far, nanochannel titania membrane,¹⁰ mesoporous silicas,¹¹ carbon nanotubes and mesoporous carbons,^{12,13} nanoparticles or nanocomposite,¹⁴⁻¹⁷ block copolymer membranes,¹⁸ etc. have been used for adsorbing or separating proteins. Although nanoporous carbons have providing a new platform for the separation of proteins,^{13,19-21} it is difficult to directly apply in large scale system because some

flaws still exist for fabrication of mesoporous carbon such as complexity, high cost and toxicity.

Banana peel (BP), as a common biomass waste, which have abundant chemical groups including carboxyl, hydroxyl and amide groups,²² would be easily modified and assembled with various chemicals.²³⁻²⁵ In this work, an inexpensive carbonaceous adsorbent with intestine-like mesostructure was fabricated through chemically modifying BP and applied to size-selective isolation of proteins.

Experimental

Materials and Chemicals.

Crude BP was obtained from a local fruit market in Xi'an, China and thoroughly washed by distilled water for further use. Commercial triblock copolymers, Pluronic F127 (Poly(ethylene oxide)-block-poly(propylene oxide)-block-poly(ethylene oxide), PEO₁₀₆PPO₇₀PEO₁₀₆, $M_w = 12600$) was purchased from Sigma-Aldrich Corp. Al(NO₃)₃·9H₂O, NaOH, hydrofluoric acid (HF), Na₂CO₃, NaHCO₃, and ethanol were purchased from the Sinopharm Chemicals Co., Ltd (Shanghai, China). Cytochrome c (Cyt c, purity>98%), bovine serum albumin (BSA, purity>98%) and lysozyme (Lyz, purity>98%) were purchased from Sigma-Aldrich Corp. All chemicals were of analytical grade and used without further purification. Ultra-pure water (18.2 MΩ·cm) was produced by a Millipore purification system (Millipore, MA, USA) and used to prepare all aqueous solutions.

Fabrication of intestine-like micro/mesoporous carbon

Intestine-like micro/mesoporous carbon (ILMC) was fabricated referencing the previous method with some modifications.²⁵ Briefly, about 2 kg BP was washed and cut into small pieces, and then completely submerged in a 2 L of aluminum nitrate aqueous solution (1.0 mol L⁻¹) for 5 days at 100 °C. As a result, the

resulting macroscopic porous framework complexes (MPFC) were obtained. Subsequently, about 10 g MPFC was impregnated into 50 mL of F127 (2.0 g) ethanol solution for 15 h at room temperature, and then further subjected to thermo-polymerization at 130 °C for 7 h in a vacuum drying oven, and finally the multiple components co-assembled into yellow gel-like composites. Finally, the gel-like composites were heated under N₂ to 500 °C with a heating rate of 1 °C min⁻¹, then maintained at 500 °C for 2 h to decompose the surfactant of F127, and subsequently heated to 650 °C with a heating rate of 3 °C min⁻¹ and kept at 650 °C for 4 h. The obtained black monoliths were ground and immersed in 15 wt% HF for 24 h to remove the Al component. The black precipitates were washed with deionized water and dried for 24 h at 100 °C.

15 Characterizations

A Bruker Tensor 27 spectrometer with the KBr pellet technique was used to measure the infrared spectroscopy (FTIR) ranging from 400 to 4000 cm⁻¹. A Rigaku D/Max-3C X-ray diffractometer with Cu Kα₁ radiation ($\lambda = 1.54 \text{ \AA}$) was applied to measuring the X-ray diffraction (XRD) pattern at 40 kV and 30 mA with an Inel CPS 120 hemispherical detector. The FEI Quanta 200 scanning electron microscope was used to obtain the scanning electron microscopy (SEM) images at an accelerating voltage of 20 kV. A JEOL JEM-2100 microscope was used to obtain the transmission electron microscopic (TEM) images at 200 kV. Samples were first dispersed in ethanol and then collected using carbon-film-covered copper grids for analysis.

The Micromeritics ASAP 2020 volumetric adsorption analyzer was employed to measure nitrogen sorption isotherms at 77 K. Prior to analysis, the sample was automatically and manually degassed for 9 h and 4 h under vacuum at 523 K, respectively. The sample was then transferred to the analysis system cooled in liquid nitrogen. The specific surface area was calculated by the Brunauer-Emmett-Teller (BET) equation based on the adsorption data at a relative pressure range of 0.05 to 0.3; the total pore volume was evaluated by converting the adsorption volume of nitrogen at relative pressure of 0.976 to equivalent liquid volume of the adsorbate, while the micropore volume were obtained by using the t-plot method. Pore size distributions were determined from the adsorption branches of the isotherms using nonlocal density functional theory (NLDFT) model.

Zeta potential measurement

The point of zero charge (pH_{PZC}) was carried out according to the previous report.²⁶ Briefly, the ILMC (0.15 g) was added into the 50 mL 0.1 M KNO₃ solution by adjusting the pH values between 2 and 12 with 1 M HCl or 1 M NaOH, and the final pH was measured after 48 h under agitation in triplicate. The difference between the initial (pH₀) and final pH (pH_f) values ($\Delta\text{pH} = \text{pH}_f - \text{pH}_0$) was plotted against the pH₀. The point of intersection of the resulting curve with abscissa, at which $\Delta\text{pH} = 0$, gave the pH_{PZC}.

Isolation of protein

The size-selective isolation of proteins on ILMC were investigated in the binary mixtures of Cyt c and BSA, Lyz and Cyt c, and the ternary mixture of BSA, Lyz and Cyt c systems. In each adsorption trial, 50.0 mg of ILMC was suspended in 20 mL

bicarbonate buffer solution (pH 9.6) with a certain concentration of proteins, respectively. The resulting mixture was continuously shaken for 16 h at 130 rpm until equilibrium was reached at 303 K. The mixture was centrifuged for 4 min at 2500 g. The relative percentage of protein adsorbed was measured by UV absorption at 409 nm for Cyt c, and at 280 nm for BSA and Lyz.

Results and discussion

Characterizations of ILMC

FTIR spectrum of ILMC displayed some typical adsorption peaks (Fig. 1a), which including the broad band at 3420 cm⁻¹ is related to O-H groups, 1618 cm⁻¹ is assigned to C=O stretching of carboxylic acid or ester and 1384 cm⁻¹ is identical to COO⁻ anion stretching.²³ XRD spectrum of ILMC displayed two adsorption peaks at $2\theta \approx 25$ and 44° (Fig. 1b), which were attributed to the (002) and (100) diffractions for graphitized carbon.²⁷ In addition, the pH_{PZC} of ILMC was measured using the acid/base titration method, and the pH_{ZPC} was ca. 5.2 (Fig. 1c).

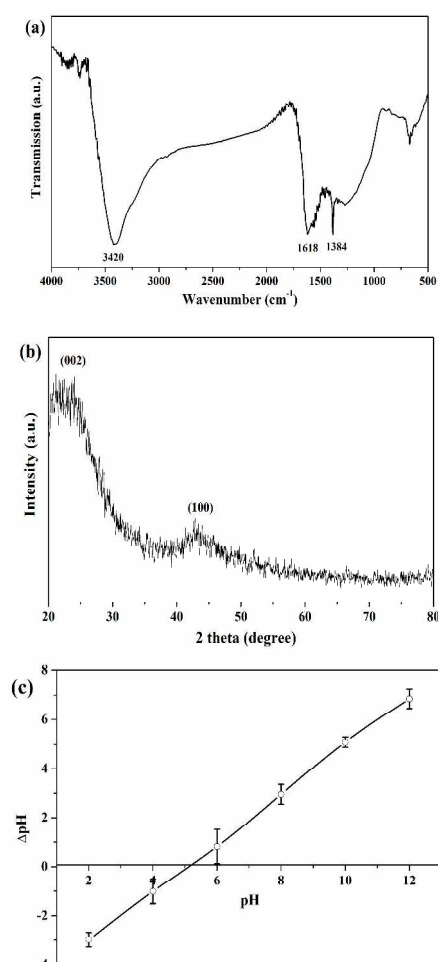


Fig. 1. FTIR spectrum (a), XRD pattern (b) and point of zero charge (c) of ILMC.

The SEM images showed that the surface of ILMC exhibits a well pronounced intestine-like structure, with a series of irregular

cavities distributed around the cross section (Fig. 2a-c). The TEM image showed that the ILMC material has abundant 2D nanoporous textures (Fig. 2d-h), which can provide a rapid transfer channel of molecules through the mesostructure.

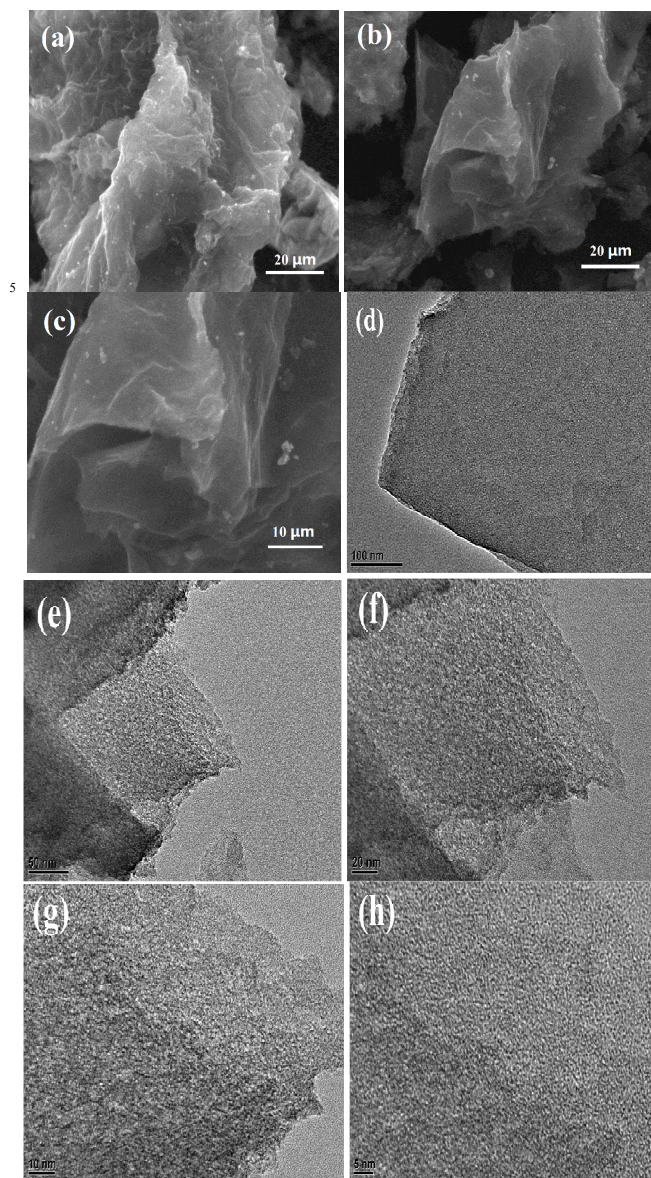


Fig. 2. SEM (a-c) and TEM (d-h) images of the sample ILMC.

As shown in Fig. 3a, the nitrogen sorption isotherm features an intermediate between type I and type-IV curves with a sharp capillary condensation step in the relative pressure range of 0.4-0.6 and H1-type hysteresis loop, indicative of uniform cylindrical pores in size range of mesoporous. The steep increase in the adsorbed volume at low relative pressure was related with the presence of micropores, the desorption hysteresis at medium relative pressure revealed the existence of developed mesopores.²⁸ The pore size distribution of ILMC was ascertained by the NLDFT model, which is mainly distributed between 0.5 and 20 nm (Fig. 3b and Table 1), with an average pore size of 2.60 nm. This finding shows that the vast majority of the pores fall into the range of mesoporous for ILMC.

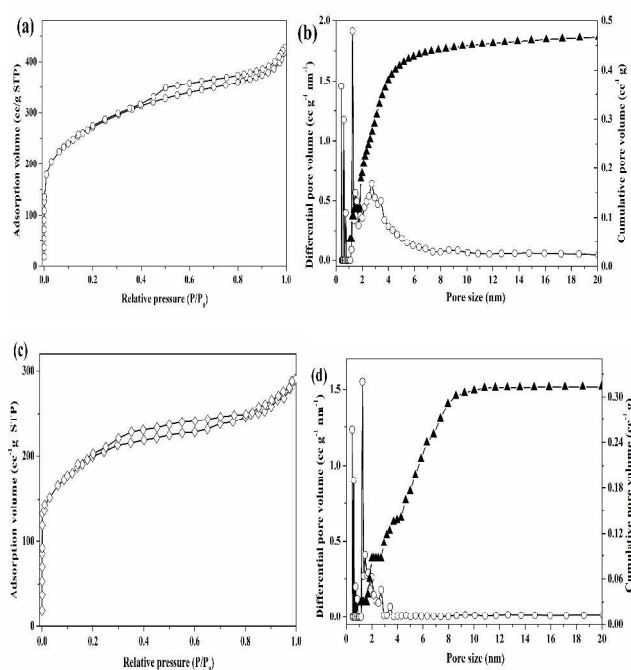


Fig. 3. Nitrogen sorption isotherms, cumulative pore volumes and pore size distributions of ILMC before (a, b) and after (c, d) adsorbing Cyt c from a ternary solution of Cyt c, BSA and Lyz.

Table 1. Porosity structures of the ILMC prepared from BP

Properties	ILMC
BET surface area ($\text{m}^2 \text{g}^{-1}$)	995
Langmuir surface area ($\text{m}^2 \text{g}^{-1}$)	1364
Total pore volume (cc g^{-1})	0.63
Micropore volume (cc g^{-1})	0.22
Mesopore volume (cc g^{-1})	0.41
Average pore size (nm)	2.60
Average mesoporous size (nm)	3.55

Isolation of protein

To explore the as-prepared ILMC as a new protein adsorbent in size-selective isolation, three typical proteins with different molecular sizes, including Cyt c (MW 12.3 kDa, pI 9.8, molecular dimensions $2.6 \times 3.2 \times 3.0 \text{ nm}$),^{29,30} BSA (MW 66.4 kDa, pI 4.8, molecular dimensions $4.0 \times 4.0 \times 14 \text{ nm}$)^{31,32} and Lyz (MW 14.4 kDa, pI 11.2, molecular dimensions $3.0 \times 3.0 \times 4.5 \text{ nm}$),^{31,33} were chosen as model molecules (Fig. 4). The relative percentage of protein adsorbed was used for evaluating the adsorption efficiency.

Owing to the adsorption capacity could be maximized near the pI,^{11,34} the adsorption at near the isoelectric point was firstly investigated for Cyt c, BSA and Lyz at pH 9.6, pH 4.8 and pH 11.2, respectively. The corresponding results (Fig. 5) showed that the adsorptions of ILMC were poor for BSA ($7.80 \pm 0.12\%$, $n = 3$) and Lyz ($6.61 \pm 0.17\%$, $n = 3$), while the adsorption for Cyt c ($63.87 \pm 0.19\%$, $n = 3$) was very strong. The results mainly attributed to the dimensions of BSA and Lyz are larger than the average mesoporous pore size of ILMC (approximately 3.55 nm), most of BSA and Lyz were excluded from the pores of the

adsorbent. The dimension of Cyt c is lower than the average mesoporous pore size of ILMC, thus the maximal adsorption was acquired. This indicates that the size selectivity is excellent by using ILMC with a narrow mesopore size distribution as an adsorbent to separate Cyt c at pH 9.6.

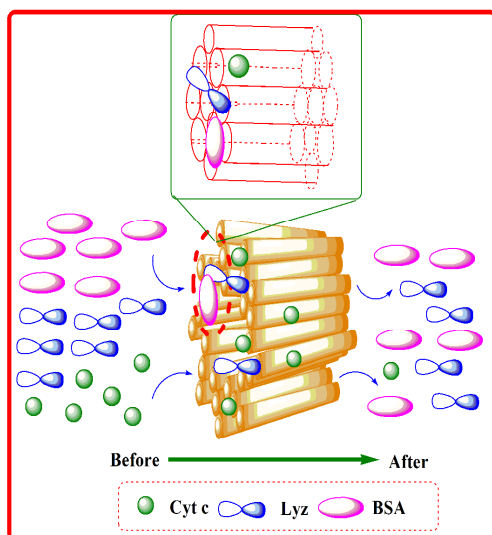


Fig. 4. Schematic of the ILMC toward selective adsorption of Cyt c among BSA (pink ellipsoid), Lyz (blue dumbbell-shaped) and Cyt c (green sphere) at pH 9.6.

The adsorption of Cyt c is typically determined by electrostatic and hydrophobic interactions.¹¹ Because the net charge of Cyt c is very low at pH 9.6, which resulted in the electrostatic repulsion between the amino acid residues on the surface of Cyt c molecules being minimal, the Cyt c molecules can be adsorbed into the pores of the ILMC by hydrophobic interactions.

In order further to understand the influence of electrostatic interaction between adsorbent and protein in size-selective isolation of Cyt c, the adsorption trials were operated for BSA and Lyz at pH 9.6, respectively. The results showed that the adsorption of ILMC for BSA presented relatively poor efficiency ($5.76 \pm 0.18\%$, $n = 3$) than that at pI (Fig. 5a), while the adsorption for Lyz ($11.43 \pm 0.23\%$, $n = 3$) was markedly more than that at pI (Fig. 5b). It could be explained as the electrostatic repulsion between the carbon surface (pI ≈ 5.2 , negative charge) and BSA molecules (negative charge) at pH 9.6 leads to negative adsorption of BSA. As for Lyz, it held a little positive charge at pH 9.6, this makes more contribution to the adsorption of Lyz on ILMC. In addition, Lyz has a prolate spheroid shape with two characteristic cross sections: a side of dimensions roughly 3.0×4.5 nm and an end of dimensions 3.0×3.0 nm,³³ so the size of part of Lyz could be match the pores of the adsorbent and resulted in more electrostatic adsorption. Higher percentage of adsorbed Cyt c at pH 7.4 ($75.02 \pm 0.26\%$, $n = 3$) than that at pH 9.6 (Fig. 5c) further demonstrated that electrostatic interaction between adsorbent and protein effected the adsorption capacity.

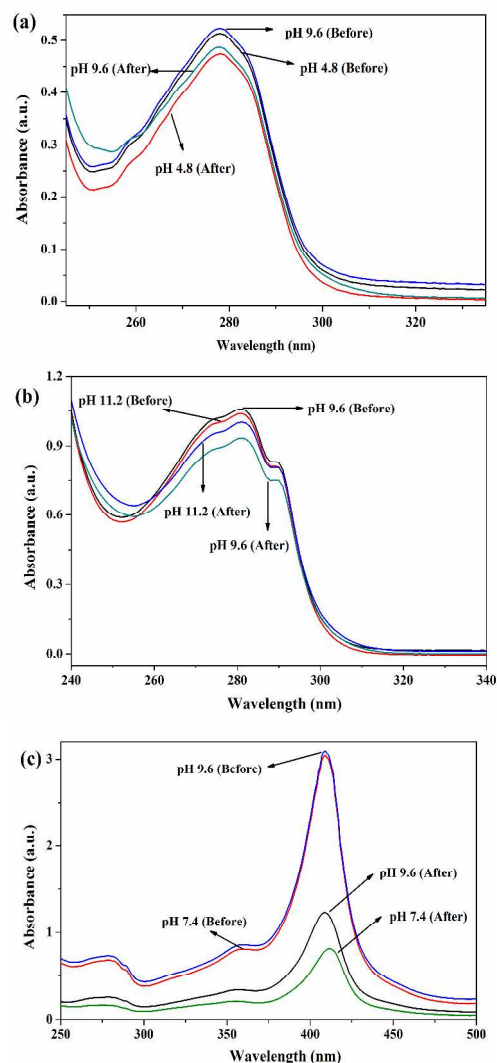


Fig. 5. UV-Vis spectra of protein solutions before and after being adsorbed on ILMC. (a) BSA (0.6 mg mL^{-1}) at carbonate buffer solution (pH 9.6) and acetic acid buffer saline (pH 4.8); (b) Lyz (0.4 mg mL^{-1}) at carbonate buffer solution (pH 9.6) and phosphate buffer solution (pH 11.2); (c) Cyt c (0.4 mg mL^{-1}) at carbonate buffer solution (pH 9.6) and phosphate buffer solution (pH 7.4).

Considering the anchoring ability of COOH groups located inside and at the entrance of the mesoporous cavity might obstruct desorption of protein molecules from the pore channels of carboxy carbon³³ at pH 7.4, the pI of Cyt at pH 9.6 was determined to isolate Cyt c from a protein mixture solution. It could be seen that the amount of adsorbed Cyt c in the binary solution of Cyt c and Lyz (Fig. 6a) is lower than that in the binary solution of Cyt c and BSA (Fig. 6b). The difference in the selectively adsorption Cyt c from different competitive proteins might ascribe to that the interaction between Cyt c and Lyz is relatively stronger than that of Cyt c and the large protein BSA.¹¹ Fig. 6c shows the UV-Vis spectra of Cyt c, BSA and Lyz ternary mixed protein solution before and after the adsorption. The peak at 280 nm for BSA and Lyz decreased 21.63% and the peak intensity of Cyt c at 409 nm was dramatically reduced ($60.05 \pm$

0.23%, $n = 3$) after adsorption, indicating that Cyt c is more easily adsorbed on ILMC than BSA and Lyz. Such selectivity is mainly attributed to numerous large accessible mesopores and the high surface area of ILMC. For better comparison, the commercial activated carbon as a representative micropore matrix was investigated for the adsorption of ternary mixed protein solution, and the result indicated that the selective to Cyt c was very poor (data no shown). This further demonstrated that the adsorption selective of ILMC to Cyt c is mainly attributed to Cyt c having a smaller spherical size than the ILMC mesopore window

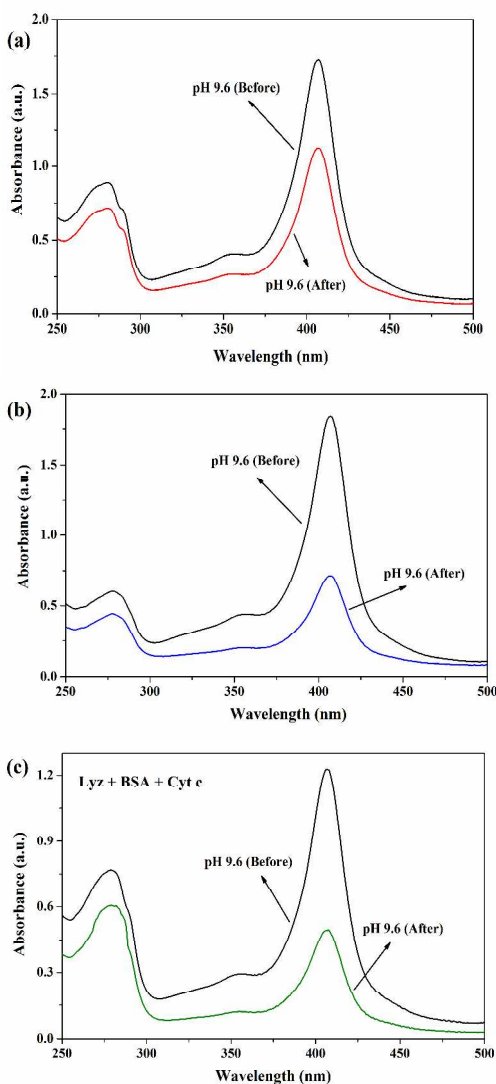


Fig. 6. UV-Vis spectra of binary and ternary protein solutions (pH 9.6) before and after being adsorbed on ILMC. (a) Cyt c (0.2 mg mL^{-1}) and Lyz (0.2 mg mL^{-1}); (b) Cyt c (0.2 mg mL^{-1}) and BSA (0.3 mg mL^{-1}); and (c) Cyt c, Lyz and BSA (0.13 mg mL^{-1} , respectively).

Verification for size selective isolation of proteins

To better validate whether Cyt c molecule enters the mesopore of ILMC, the adsorbent was characterized by nitrogen adsorption before and after Cyt c adsorption (Fig. 3a-d). As expected, the amounts of nitrogen adsorbed (from 428 to 298 cc g^{-1}), specific

surface areas (from 995 to 518 $\text{m}^2 \text{g}^{-1}$) and total pore volumes (from 0.63 to 0.42 cc g^{-1}) of ILMC are decreased after Cyt c adsorption. These numerical values clearly indicate that the Cyt c molecules are adsorbed inside the intestine-like mesopore of ILMC, however without affecting the structural integrity of the parent material.

Conclusions

In this work, for the first time, an ILMC with high surface area ($995 \text{ m}^2 \text{g}^{-1}$), large pore volumes (0.63 cc g^{-1}), and narrow mesopore size distribution (ca. 3.55 nm) was fabricated through chemically modifying BP and successfully used for selective isolation of Cyt c from mixed protein solution of BSA, Lyz and Cyt c. The findings revealed that the pore sizes of ILMC played a key role in the selective adsorption of Cyt c from mixed protein solution, associated with the electrostatic and hydrophobic interactions as well. This cheap carbonaceous adsorbent offers a very useful medium to separate biomolecules with different molecular sizes. It is believed that further development of this carbon material would benefit to the controlled release, biosensing, nanocarriers and so on.

Acknowledgements

This project was supported by the National Natural Science Foundation of China (21275098) and the Fundamental Research Funds for the Central Universities (GK201304003).

Notes and references

^a Key Laboratory of Analytical Chemistry for Life Science of Shaanxi Province, School of Chemistry and Chemical Engineering, Shaanxi Normal University, Xi'an 710062, China.

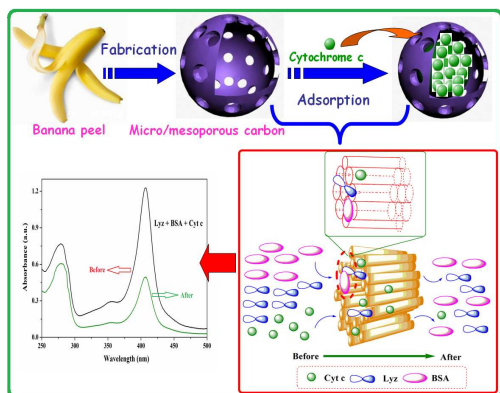
^b Key Laboratory of Medicinal Resource and Natural Pharmaceutical Chemistry (Shaanxi Normal University), Ministry of Education, Xi'an 710062, China.

Fax: 86-29-81530792; E-mail: zqzhang@snnu.edu.cn (Z.-Q. Zhang)

- M. Hu, J. Reboul, S. Furukawa, N. L. Torad, Q. Ji, P. Srinivasu, K. Ariga, S. Kitagawa and Y. Yamauchi, *J. Am. Chem. Soc.*, 2012, **134**, 2864-2867.
- N. Fechner, T.-P. Feller and M. Antonietti, *Adv. Mater.*, 2013, **25**, 75-79.
- B. Hu, K. Wang, L. Wu, S.-H. Yu, M. Antonietti and M.-M. Titirici, *Adv. Mater.*, 2010, **22**, 813-828.
- B. Hu, S.-H. Yu, K. Wang, L. Liu and X.-W. Xu, *Dalton Trans.*, 2008, **40**, 5414-5423.
- K. Y. Foo and B. H. Hameed, *Bioresour. Technol.*, 2012, **104**, 679-686.
- H. Bi, Z. Yin, X. Cao, X. Xie, C. Tan, X. Huang, B. Chen, F. Chen, Q. Yang, X. Bu, X. Lu, L. Sun and H. Zhang, *Adv. Mater.*, 2013, **25**, 5916-5921.
- X.-L. Wu, T. Wen, H.-L. Guo, S. Yang, X. Wang and A.-W. Xu, *ACS Nano*, 2013, **7**, 3589-3597.
- R. J. White, V. Budarin, R. Luque, J. H. Clark and D. J. Macquarrie, *Chem. Soc. Rev.*, 2009, **38**, 3401-3418.
- A. Vinu, M. Masahiko, V. Sivamurugan, T. Mori and K. Ariga, *J. Mater. Chem.*, 2005, **15**, 5122-5127.
- P. Roy, T. Dey, K. Lee, D. Kim, B. Fabry and P. Schmuki, *J. Am. Chem. Soc.*, 2010, **132**, 7893-7895.
- M. Zhang, Y. Wu, X. Feng, X. He, L. Chen and Y. Zhang, *J. Mater. Chem.*, 2010, **20**, 5835-5842.
- X. Chen, L. Hu, J. Liu, S. Chen and J. Wang, *Trac.-Trend. Anal. Chem.*, 2013, **48**, 30-39.

13. D. Feng, Y. Lv, Z. Wu, Y. Dou, L. Han, Z. Sun, Y. Xia, G. Zheng and D. Zhao, *J. Am. Chem. Soc.*, 2011, **133**, 15148-15156.
14. F. Gao, H. Qu, Y. Duan, J. Wang, X. Song, T. Ji, L. Cao, G. Nie and S. Sun, *RSC Adv.*, 2014, **4**, 6657-6663.
- 5 15. N. Sankarakumar and Y. W. Tong, *RSC Adv.*, 2013, **3**, 1519-1527.
16. F. Lan, Y. Wu, H. Hu, L. Xie and Z. Gu, *RSC Adv.*, 2013, **3**, 1557-1563.
17. J. Kim, Y. Piao, N. Lee, Y. I. Park, I.-H. Lee, J.-H. Lee, S. R. Paik and T. Hyeon, *Adv. Mater.*, 2010, **22**, 57-60.
- 10 18. J. Hahn, J. I. Clodt, V. Filiz and V. Abetz, *RSC Adv.*, 2014, **4**, 10252-10260.
19. T. N. Shah, H. C. Foley and A. L. Zydney, *J. Membrane Sci.*, 2007, **295**, 40-49.
20. H. Qin, L. Zhao, R. Li, R. Wu and H. Zou, *Anal. Chem.*, 2011, **83**, 7721-7728.
- 15 21. Z. Sun, Y. Liu, B. Li, J. Wei, M. Wang, Q. Yue, Y. Deng, S. Kaliaguine and D. Zhao, *ACS Nano*, 2013, **7**, 8706-8714.
22. C. Liu, H. H. Ngo, W. Guo and K.-L. Tung, *Bioresour. Technol.*, 2012, **119**, 349-354.
- 20 23. Y. Lv, L. Gan, M. Liu, W. Xiong, Z. Xu, D. Zhu and D. S. Wright, *J. Power Sources*, 2012, **209**, 152-157.
24. C. R. Silva, T. F. Gomes, G. C. R. M. Andrade, S. H. Monteiro, A. C. R. Dias, E. A. G. Zagatto and V. L. Tornisielo, *J. Agric. Food Chem.*, 2013, **61**, 2358-2363.
- 25 25. R.-L. Liu, Y. Liu, X.-Y. Zhou, Z.-Q. Zhang, J. Zhang and F.-Q. Dang, *Bioresour. Technol.*, 2014, **154**, 138-147.
26. A. Kumar, B. Prasad and I. M. Mishra, *J. Hazard. Mater.*, 2008, **152**, 589-600.
27. P. Pachfule, V. M. Dhavale, S. Kandambeth, S. Kurungot and R. Banerjee, *Chem. Eur. J.*, 2013, **19**, 974-980.
- 30 28. B. Liu, H. Shioyama, T. Akita and Q. Xu, *J. Am. Chem. Soc.*, 2008, **130**, 5390-5391.
29. Z. Sun, Y. Deng, J. Wei, D. Gu, B. Tu and D. Zhao, *Chem. Mater.*, 2011, **23**, 2176-2184.
- 35 30. M. Matsui, N. Takahashi and J.-i. Ozaki, *Carbon*, 2011, **49**, 4505-4510.
31. A. Katiyar and N. G. Pinto, *Small*, 2006, **2**, 644-648.
32. X. Qiu, H. Yu, M. Karunakaran, N. Pradeep, S. P. Nunes and K.-V. Peinemann, *ACS Nano*, 2013, **7**, 768-776.
- 40 33. A. Vinu, K. Z. Hossian, P. Srinivasu, M. Miyahara, S. Anandan, N. Gokulakrishnan, T. Mori, K. Ariga and V. V. Balasubramanian, *J. Mater. Chem.*, 2007, **17**, 1819-1825.
34. I. I. Slowing, B. G. Trewyn and V. S.-Y. Lin, *J. Am. Chem. Soc.*, 2007, **129**, 8845-8849.

Table of content entry



An intestine-like nanoporous carbon was fabricated and used for size-selective separation of cytochrome c.

5